J4.8 INFLUENCE OF HYDROLOGIC MEMORY ON TERRESTRIAL IMPACTS OF ENSO

Praveen Kumar* and Ji Chen
University of Illinois, Urbana, Illinois

ABSTRACT

Relationships between the terrestrial hydrologic processes over the North American continent and the El Niño/Southern Oscillation (ENSO) are investigated using a large area basin-scale (LABs) land surface model driven by European Centre for Medium-Range Weather Forecasts Re-Analyses 15-year (ERA-15) dataset.

It is found that the terrestrial systems have both short and long term delayed responses to the ENSO signals, as compared to the precipitation. The shorter and longer delays are typically associated with rainfall runoff, and snow accumulation and melt processes, respectively. The soil moisture storage plays a very vital role in delaying the effects of the climate variability on the terrestrial hydrologic processes and in extending the influences of the El Niño or La Niña events on the terrestrial climate. It is also found that the fluctuations of the soil temperature anomalies at different soil depths, in certain geographic regions, are correlated with the ENSO signal, and the strength and the associated time lag of this correlation increase with increasing soil depth.

1 INTRODUCTION

ENSO has important impacts on various terrestrial systems (Glantz 2001). The influence on the hydrologic system serves to transmit the climate signal to several of these terrestrial systems. Consequently, our ability to model and predict the terrestrial hydrologic response to ENSO will provide significant advancement in several related areas of research.

In this paper we present a modeling study using the LABs model (Chen and Kumar 2001) to understand the response of the terrestrial hydrologic variables to ENSO. We use the results from a 15-year model simulation (1979-1993) using ERA-15 dataset (Gibson et al. 1999) and study the lagged cross-correlation of the ENSO index with the anomalies of several model variables.

* *Corresponding author address:* Prof. Praveen Kumar, Environmental Hydrology and Hydraulic Engineering, Department of Civil and Environmental Engineering, University of Illinois at Urbana-Champaign, Urbana, Illinois 61801; e-mail:kumar1@uiuc.edu.

2 BACKGROUND

Large area basin scale (LABs) model (Chen and Kumar 2001) combines the vertical moisture and energy transport of NCAR LSM (Bonan 1996) and runoff generation of Topmodel (Beven and Kirkby 1979). All processes are simulated at the basin scale; each basin is treated as a column with 6 soil layers. The North American continent is divided into 5020 basins using the HYDRO1K data (Verdin and Verdin 1999) with an average basin size of 3255 km^2. A two year spin-up cycle is used for initializing the model. The simulation time step is 30 minutes.

We derive the ENSO index from the raw data of NOAA (National Oceanic and Atmospheric Administration) Niño 3 SST for the base climatologic period of 1979-1993 (see Fig. 4(top)).

3 METHODOLOGY

The ERA-15 forcing and the model output are combined into the monthly aggregates and anomalies for correlation with the ENSO index. The monthly mean of a variable of interest is computed. The complete 15-year monthly anomaly series is obtained with monthly mean removed. The sample size of the anomaly series is 180 for a 15-year dataset. For the single monthly 15-year dataset which group the same months together, for each month there is a series of 15 values corresponding to each year. For the single anomaly series, the correlation coefficient between the anomaly of each terrestrial variable and ENSO index is computed. The relationship between the complete anomaly series and the ENSO signal is studied by computing and analyzing their cross-correlation coefficient and the time lag associated with the extremal value of the cross-correlation coefficient.

In order to locate the significant correlation areas, we use the t-test statistic to identify the confidence interval of the correlations between ENSO and the terrestrial hydrologic variables.

4 RESULTS

4.1 *Teleconnection Between ENSO and Terrestrial Hydrology*

4.1.1 Runoff

The extremal cross-correlation between the ENSO index and the anomaly of the runoff over North America (Fig. 1(a)) shows that there are three distinct coherent negatively-correlated regions: center of Canada, northwestern Alaska and South Mexico. These regions will henceforth be referred to as the CD, AL and MX regions. The runoff anomalies in the north and northwest regions of the North American continent are most often negatively-correlated with the ENSO signal.

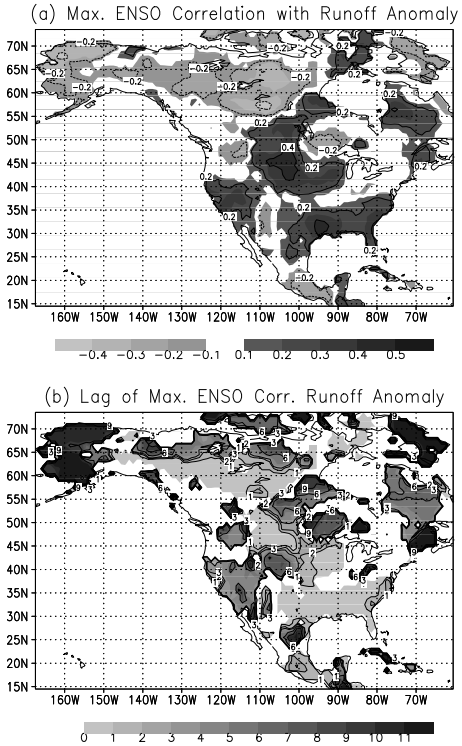

Figure 1: (a) Extremal cross-correlation coefficient between ENSO and model simulated runoff anomalies for each basin. (b) Associated monthly lag.

In contrast, there are four distinct positively-correlated regions: center of the continent, area around the Gulf of Mexico, area around the Hudson Bay and area around California and Nevada. These four regions will be referred to as the CN, GM, HB and CA regions, respectively (see Fig. 2). When considering the lag corresponding to the extremal correlation (Fig. 1(b)), it is more than six months in the high land of the Rocky Mountains in the CN region. The maximum correlation in the east of the in GM region has a one or two month lag with respect to ENSO. The time lag in the CA region is about a season long.

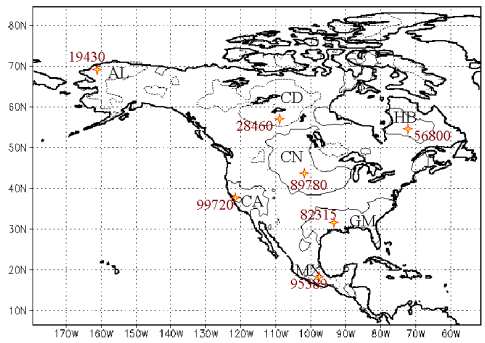

Figure 2: Seven distinct ENSO correlation regions. Three of them, CD, AL and MX, are negatively correlated, and the rest, CN, GM, HB and CA, are positively correlated. The seven star marks and numbers are the locations and basin IDs. These basins are chosen for detailed study (see Table 1).

The negatively-correlated region in the CD region demonstrates a high probability of low flow during the warm phase of an ENSO year and/or of high flow during the cool phase. The four positively-correlated regions have high flow potential in an El Niño year and/or low flow potential in a La Niña year. The spring and summer drought of 1988 over the central United States associated with La Niña and the summer flood of 1993 in the U.S. Midwest associated with the mature El Niño conditions (Trenberth and Guillemot 1996) are mostly located in the CN region.

4.1.2 Precipitation

The forcing variable directly related to a basin's runoff is precipitation. Figure 3 displays the extremal cross-correlation coefficient between ENSO and the precipitation anomaly for each basin and the associated time lag. The spatial correlation pattern for precipitation is similar to that of runoff; however, the correlation with the runoff anomaly is stronger. In addition, the time lag for the runoff anomaly is, in certain areas, longer than that for the precipitation anomaly by one or two months. In areas where runoff is primarily associated with snowmelt, such as the area around Wyoming, the lag differences are more than five or six months.

4.2 *Teleconnection Lags*

From the above analysis it is evident that the terrestrial systems have a delayed response to the ENSO signals, as compared to the precipitation. To verify that the correlation and the computed lags are not a computational or statistical artifacts, seven

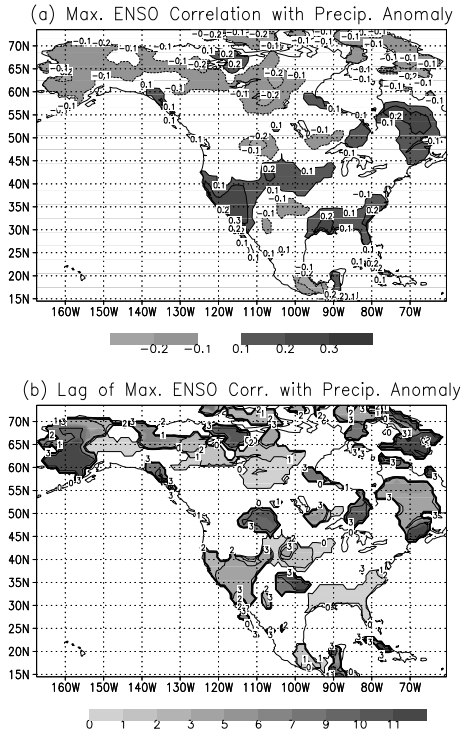

Figure 3: Same as Fig. 1 but for precipitation.

basins corresponding to the center of each region (Table 1, Fig. 2) are chosen for a detailed study. These basins correspond to the centers of the seven regions with distinct coherent correlations between ENSO and runoff anomalies. The product of ENSO index $E(t)$ and the lagged time series $y'(t + \tau_{max})$, where y' is runoff anomaly (Fig. 4), or precipitation anomaly (Fig. 5), illustrates that the lags of extremal correlations are indeed important in teleconnection patterns. Although there are only five ENSO events in the 15 year study period, the correlation method is effective in identifying the influence of ENSO on the runoff response (Fig. 4) which do show markedly different characteristics during this period. The 1982-1983 El Niño and 1988-1989 La Niña have strong signatures in basins with positive and negative correlations, respectively. In addition, basin 99720, located in the CA region, shows a very strong correlation with the 1982-1983 event and the contribution to the correlation value during the 15-year period is primarily because of this event. This is also indicative of the fact that the regions identified as correlated with ENSO events are not necessarily affected by every episode.

The analysis of the precipitation anomaly (Fig. 5) indicates that the precipitation during ENSO episodes is generally different from other periods.

Table 1: Seven basins, from four positively and three negatively ENSO correlated regions over North America (see Fig. 2), are chosen for detailed study.

Region	Basin ID	Latitude ddmmss	Longitude dddmmss	ENSO Phase
CN	89780	431941N	1014120W	+
GM	82315	315817N	0932947W	+
HB	56800	542746N	0714647W	+
CA	99720	385216N	1225447W	+
CD	28460	572215N	1092700W	-
AL	19430	680230N	1602039W	-
MX	95389	181651N	0972859W	-

Figure 4: Product time series of ENSO index ($E(t)$, top) and monthly runoff anomalies (RA) from seven basins identified in Fig. 2. ENSO index (top) is relative to the base period climatologies of 1979-1993, and the horizontal thick dash lines represent $\pm 0.5^{\circ}$C indicate a threshold band, exceeder of which corresponds to a ENSO condition.

In addition, the precipitation time series is more variable as compared to the runoff which partly explains the lower correlation coefficients, as compared to runoff. These results also support the argument that even though the estimated correlations of hydrologic variables with the ENSO index are generally low, they do reflect the important teleconnection

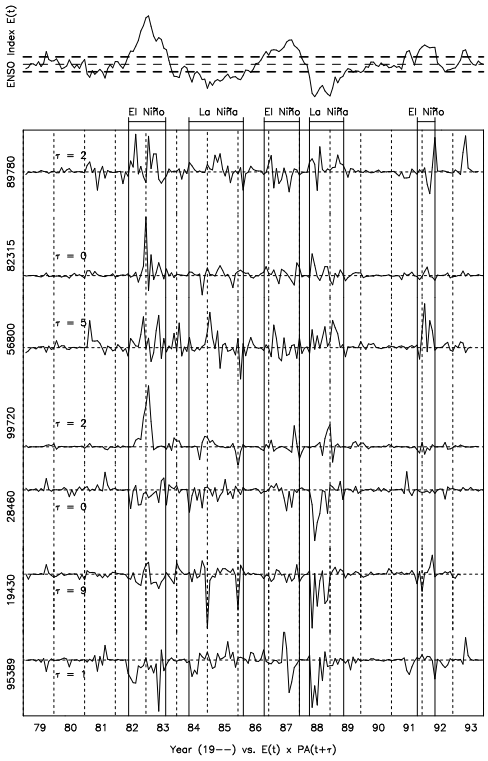

Figure 5: Same as Fig. 4 but for monthly precipitation anomalies (PA).

impacts and the observed regional patterns are not spurious.

4.3 *Soil Moisture Storage and Terrestrial Climate*

To understand the role of soil moisture storage in determining terrestrial climate, two categories of soil water deficit are considered in the study. First is total soil water deficit (TSWD). The second is the near-surface soil water deficit (NSWD) which refers to the soil water deficit in the first soil layer, with thickness 10 cm. Because the first soil layer is shallow and quickly interacts with various driving variables, NSWD reflects the rapid fluctuation of the land surface forcing from the atmosphere, and represents the short time scale memory. Meanwhile, TSWD reflects the total memory of the soil system in response to the larger time scale of the atmospheric forcing.

The corroboration of the study of relationship between ENSO and soil moisture storage is offered by examining the ENSO correlation with runoff and precipitation, and NSWD and TSWD, using the annual series for the months of June and July. In June, there is a distinct positively-correlated area for the precipitation anomaly over the CN and CA regions and the most part of GM region (Fig. 6). A corresponding pattern is identifiable for the runoff anomaly except with stronger correlation around the GM region. As compared to June, precipitation anomaly shows lower correlation in July for the GM region. However, the runoff continues to show strong correlation in July. The TSWD continues to show strong correlation in July (Fig. 7) while the pattern for NSWD anomaly is more reminiscent of that of precipitation. In June, the location of the negative correlation between ENSO and the TSWD anomaly closely matches that of ENSO and the runoff anomaly. In addition, the area of the correlation between ENSO and the NSWD anomaly has not only the signature of the precipitation anomaly but also that of the TSWD anomaly. In July, the correlation area around the GM region for the TSWD anomaly shrinks and the correlation strength decreases, and the correlation area around the CN region enlarges and the correlation strength increases. Moreover, the correlation area around the GM region for the NSWD anomaly reduces dramatically and only remains a small area near the outlet of the Mississippi River. However, the area along the U.S. and Canada border with high correlation between ENSO and the precipitation anomaly also shows the distinct correlation between ENSO and the NSWD anomaly. Clearly, the NSWD anomaly is a mix representing primarily the dynamics of precipitation but it also impacted by the total storage as characterized by TSWD.

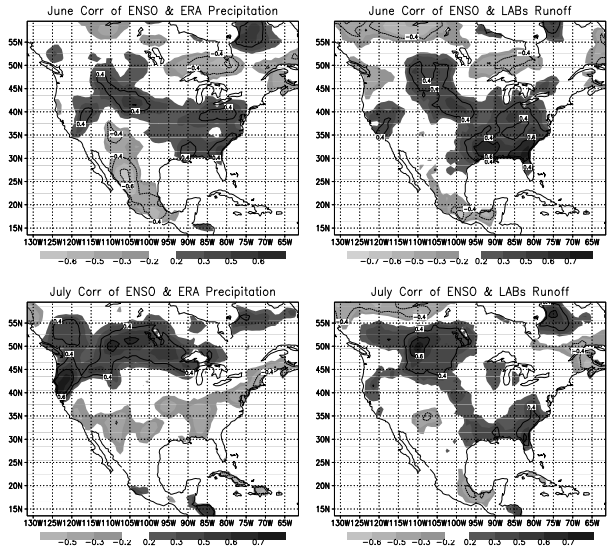

Figure 6: Monthly correlations of ENSO with ERA-15 precipitation (Left) and runoff (Right) anomalies for June (Top) and July (Bottom).

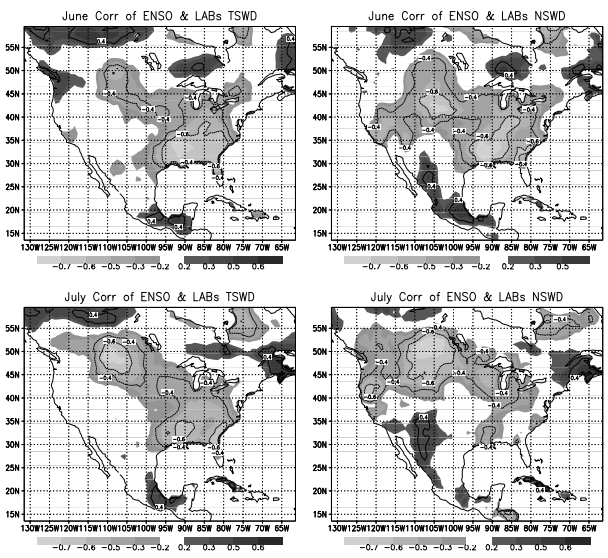

Figure 7: Monthly correlations of ENSO with model simulated TSWD (Left) and NSWD (Right) anomalies for June (Top) and July (Bottom).

4.4 *ENSO Correlation With terrestrial Energy*

Figure 8 shows the soil temperature and energy anomalies of each soil layer with ENSO index time series in basin 88490, which is in the Upper-Mississippi River basin. The left side of Fig. 8 is the soil temperature anomalies at six soil layers, and these vertical coordinates are on the same scale. In the figure, it is found that the amplitudes of soil temperature anomaly fluctuations decrease from layer one to six. Also, their frequencies decrease along the increasing soil depth. At these six soil layers, it is found that there are three wave crests corresponding to the three El Niño events and two wave trough corresponding to the two La Niña events during the fifteen year time period (see the dash lines in the left side of Fig. 8). The terrestrial heat energy storage (THES) anomaly at each soil layer is on the right side of Fig. 8. Because soil moisture anomaly at soil layer 6 doesn't have distinct fluctuation, layer six THES is determined by soil temperature and shows a similar fluctuation as soil temperature anomaly. However, at soil layer 5, the THES anomaly doesn't reflect soil temperature anomaly and is primarily determined by soil moisture variation in this layer, and the largest negative energy anomaly appeared in 1988 which is consistent with the 1988 drought in this area. In other soil layers, from layers one to four, the THES anomalies are also controlled by the variations of the soil moisture anomaly rather than soil temperature anomaly.

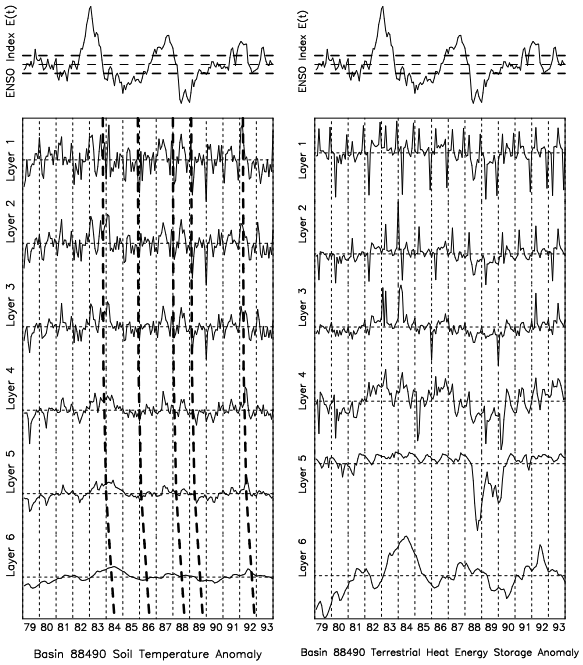

Figure 8: The ENSO index (Top) and the anomalies of soil temperature (Bottom left) and THES (Bottom right) at six soil layers in basin 88490. The dash lines schematically display the signatures of ENSO at different soil layers.

In order to further verify the relationship between terrestrial energy and ENSO, the products of ENSO and the soil temperature and THES anomalies at six soil layers in the basin are displayed in Fig. 9, and the statistic summaries of the basin are presented in Table 2. In basin 88490, we find that the strength and time lag of the extremal cross-correlation of soil temperature anomaly increase from soil layer one to six. It reflects that the impact of ENSO on the soil temperature does not diminish along increasing soil depth. This further confirms the result obtained from Fig. 8. Also, the signature of ENSO in the deep soil will be useful to explain the long-term effects of this climate phenomenon on the terrestrial hydrologic processes. According to the time lag associated with the extremal cross-correlation, we find that the correlations of the THES from soil layer one to five are not determined by soil temperature anomaly but soil moisture anomaly. In contrast, in soil layer 6, the THES anomaly is determined by soil temperature anomaly at this layer. This result is consistent with the observation from Fig. 8.

5 Summary and Conclusions

Seven distinct regions with strong coherence with ENSO are identified over the North American continent. The runoff anomalies in general show higher

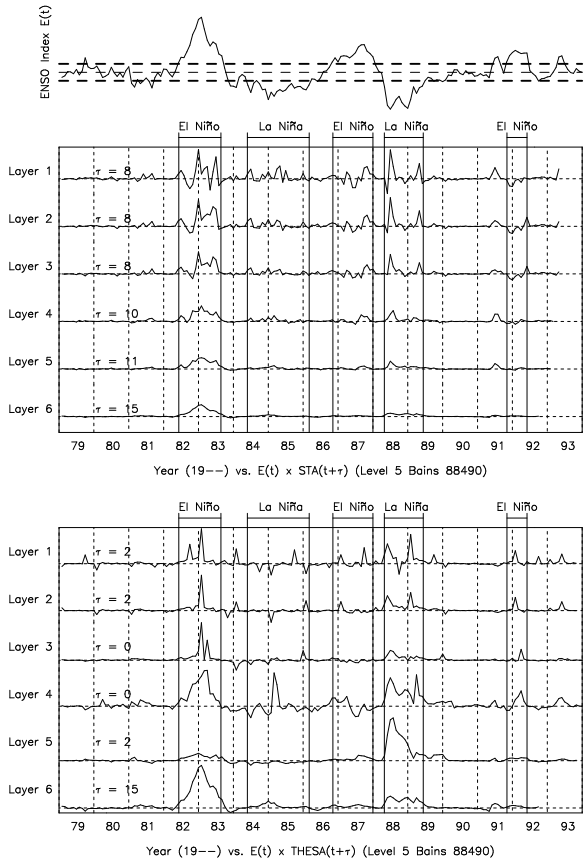

Figure 9: Products time series of ENSO index, $E(t)$ (Upper), and monthly soil temperature anomalies (STA) (Middle) and terrestrial heat energy storage anomalies (THESA) (Lower) at six soil layers in basin 88490.

Table 2: The statistics summary of the cross-correlation between ENSO and the anomalies of soil temperature and terrestrial heat energy storage of each of six soil layers in basin 88490.

	Temperature		Heat	
	Cross-Corr.	Lag	Cross-Corr.	Lag
Layer 1	0.229	08	0.248	2
Layer 2	0.339	08	0.267	2
Layer 3	0.391	08	0.327	0
Layer 4	0.506	10	0.379	0
Layer 5	0.595	11	0.467	2
Layer 6	0.647	15	0.647	15

correlation than precipitation anomalies in these regions. This is partly due lower variability of runoff time series. Also, the lag corresponding to the runoff is generally longer than that for rainfall. Regions where runoff is primarily produced by rainfall-runoff processes show shorter lags than those where snowmelt is the primary contributor to the runoff.

Study using near surface and total soil moisture deficits reveals that influence on runoff is generally communicated through the latter, while the former is more coherent with the rainfall pattern. It is hypothesized that the relatively slower dynamics of terrestrial moisture storage serves as a memory in causing the delayed peak in runoff as compared to the precipitation. In addition, the study reveals that the strength of the correlation between the ENSO signal and soil temperature increases along increasing soil depth in the certain geographic regions. This reflects the long-term effects of ENSO on the terrestrial hydrologic processes.

Acknowledgments

Support for this study has been provided by NASA Grants NAG5-3361, NAG5-8555 and NAG5-7170, and NSF Grant EAR 97-06121. Computational support was also provided by NCSA Grants EAR990004N and ATM010006N.

References

[1] Beven, K. J., and M. J. Kirkby, 1979: A physically based variable contributing area model of basin hydrology. *Hydrol. Sci. Bull.*, **24**(1), 43-69.

[2] Bonan, G. B., 1996: A land surface model (LSM version 1.0) for ecological, hydrological, and atmospheric studies: Technical Description and User's Guide. *NCAR Technical Note, NCAR/TN-417+STR*, Boulder, Colorado, 150 pp.

[3] Chen, J., and P. Kumar 2001: Topographic influence on the seasonal and inter-annual variation of water and energy balance of basins in North America. *J. Climate*, **14**(9), 1989-2014.

[4] Gibson, J. K., P. Kållberg, S. Uppala, A. Hernandez, A. Nomura, and E. Serrano, 1999: *ERA-15 description (Version 2)*. ECMWF Re-analysis Project Report Series, Part 1, ECMWF, 73 pp.

[5] Glantz, M. H., 2001: *Currents of change: Impacts of El Niño and La Niña on climate and society (Second Edition)*. Cambridge University Press, 252 pp.

[6] Trenberth, K. E., and C. J. Guillemot, 1996: Physical processes involved in the 1988 drought and 1993 floods in North America. *J. Climate*, **9**, 1288-1298.

[7] Verdin, K. L., and J. P. Verdin, 1999: A topological system for delineation and codification of the Earth's river basins. *J. Hydrol.*, **218**, 1-12.